On the Stress-Strain Response of a Deep Tunnel Under Squeezing Conditions: Numerical Analysis for the Design of Rock Supports

Gennaro Scognamiglio[1], Giulio Antonucci[1], Gianluca Bella[2-3]
[1]Italferr S.p.A., Genova, Italy
[2]Pini Group SA, Lugano, Switzerland
[3]University of Applied Sciences and Arts of Southern Switzerland (SUPSI), Mendrisio, Switzerland
g.scognamiglio@italferr.it; g.antonucci@italferr.it; gianluca.bella@pini.group

Abstract - This paper deals with a series of numerical simulations to investigate the stress-strain response of a deep tunnel under complex geo-mechanical conditions, leading to the occurrence of squeezing phenomena. The safety level resulting from different rock supports installed in the excavation stabilizations, respectively stiff or sliding ribs, is preliminarily studied. Finite element analyses are carried out by considering a circular shape tunnel under plain strain conditions, isotropic state of stress state, and elastoplastic Hoek & Brown criteria as constitutive law for the rock mass. The study covers a wide range of fracturing conditions in terms of GSI at simulating a decrease of the rock mass properties due to the proximity of tectonized zones, at giving practical suggestions to tunnel designers when excavation under squeezing rock mass conditions are foreseen.

Keywords: squeezing; deep tunnel; difficult ground conditions; sliding ribs.

1. Introduction

Squeezing rock conditions represent one of the major challenges to the construction of tunnels through mountains, as experience dating back more than a century shows. According to [1], the squeezing of rock is the time-dependent large deformation that occurs around the tunnel and is essentially associated with creep caused by exceeding a limiting shear stress. Deformation may terminate during construction or continue over a long time period. The magnitude of the tunnel convergence associated with squeezing, the rate of deformation, and the extent of the yielding zone around the tunnel depends on the geological conditions, the in situ stresses relative to rock mass strength, the groundwater flow and pore pressure, and the rock mass properties ([2]). Squeezing rock response is known to be affected by rock type and structure: in squeezing zones, the rock is strongly jointed and fractured and has low strength. Moreover, overburden has also a significant effect and squeezing behavior may occur in a tunnel once a limiting overburden has been exceeded. Several cases of squeezing occurrence during the excavation of deep tunnels are given in the literature (Fig.1), such as in the case of the Saint Martin La Porte access adit ([3]) and the Monte Ceneri base Tunnel ([4]).
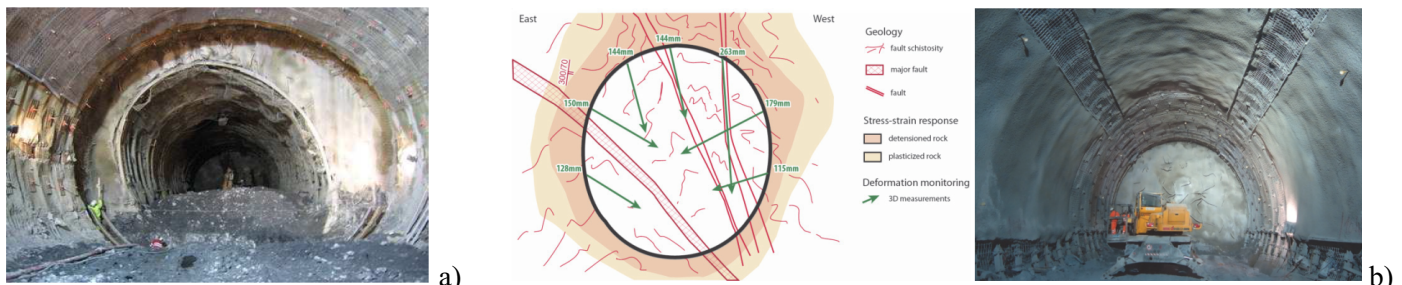
Fig. 1: a) Squeezing at S. Martin la Porte ([3]); b) Squeezing conditions with asymmetric convergences and rock-support SPV10 with yielding support and pseudo-circular shape adopted in the Val Colla Line ([4]).

Squeezing is closely related to the excavation and support techniques and sequences adopted in tunneling, so the choice of rock support is a key element in terms of safety, feasibility, and design optimizations. If the support installation is delayed,

the rock mass moves into the tunnel and a stress redistribution takes place around it. Deformable rock supports (i.e. sliding ribs) allow a certain rock mass displacement within a certain threshold, leading to a rock-mass/rock-support equilibrium to be reached, as shown in Fig.2. This stress-strain equilibrium condition is represented by the green point, which is lower than the rock support capacity. Conversely, if the rock deformations are constrained by stiff support, squeezing will lead to long-term load build-up of the support itself, and the equilibrium pressure will be reached at its limit capacity (red point) leading to possible rock support failure.
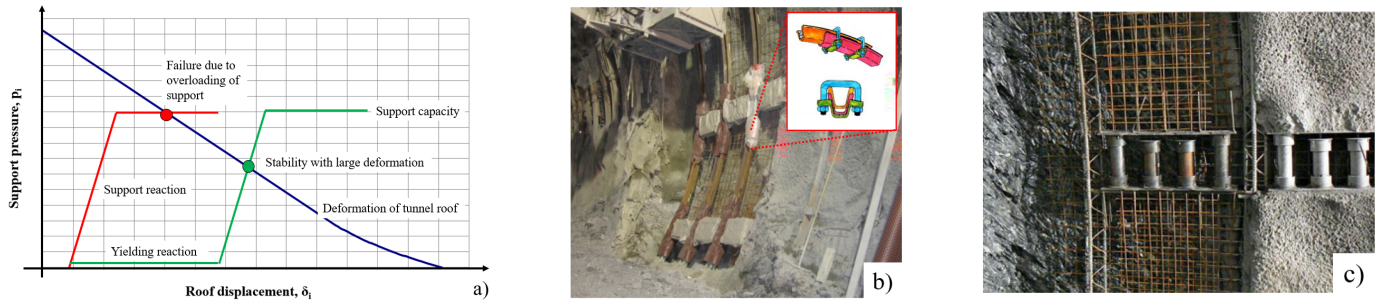
Fig. 2: a) ground reaction curve (blue) and support reaction curve for stiff ribs (red) and sliding ribs (green); b) sliding TH ribs and details; c) yielding elements with four deformation pipes ([5]).

The current study deals with the stress-strain behavior of a deep tunnel where squeezing behavior is expected. Finite element simulations are carried out by considering several fracturing states to investigate the safety level - in terms of displacement and MN domain - resulting from installing conventional rock support (stiff ribs), or sliding ribs with yielding elements as primary support.

2. Numerical simulations

2.1. General Overview

Finite element code RS2v.9.0 (RocScience) was adopted to model the transversal section of the tunnel (radius R_T=5.0m, overburden H=600m) under plane strain conditions and a constant state of stress (Fig.3). Boundary conditions consist of hinges along all sides, the model sizes were accurately set to avoid numerical side effects. Shists are supposed the rock mass within the tunnel is excavated. A certain range of MR values is suggested by [6] - [8] (shists: MR=250-1100), and an average value of MR=550 was adopted. Knowledge of the uniaxial compressive strength of the intact rock, and MR allowed to estimate the elastic modulus of the intact rock (Eqs. (1)). The deformability modulus of the rock mass (E_d) was then estimated based on Eqs. (2) proposed by [9] depending on the GSI and disturbance factor D.

$$E_i = MR \cdot UCS \tag{1}$$

$$E_d = E_i \left(0.02 + \frac{1 - D/2}{1 + e^{((60 + 15D - GSI)/11)}} \right) \tag{2}$$

The rock mass has been modeled by an elastic-perfectly plastic Hoek-Brown criterion (Table 1) by assuming an isotropic state of stress within a wide range of GSI 25-45 (analysis n.1 → analysis n.5) to simulate different fracturing conditions. Under such conditions "extreme squeezing problems" are expected according to [10].

Table 1: Rock mass parameters: unit weight (γ), geological strength index (GSI), Hoek & Brown -m_i parameter (intact rock), uniaxial compressive strength (UCS), Poisson's ratio (v), deformability modulus (E_d), rock mass strength (σ_{cm}), state of stress (p_0), earth pressure coefficient at rest (k_0).

	Analysis n.1	Analysis n.2	Analysis n.3	Analysis n.4	Analysis n.5
γ [kN/m^3]	27	27	27	27	27
GSI [-]	25	30	35	40	45
m_i [-]	20	20	20	20	20
UCS [MPa]	12	12	12	12	12
v [-]	0.30	0.30	0.30	0.30	0.30
E_d [MPa]	395	537	750	1050	1480
σ_{cm} [MPa]	0.18	0.24	0.32	0.42	0.56
p_0 [MPa]	16.2	16.2	16.2	16.2	16.2
k_0 [-]	1.0	1.0	1.0	1.0	1.0

No water table was assumed, and the tunnel excavation phases have been reproduced step-by-step, while 9'152 graded triangular elements are adopted and densified close to the relevant clusters. The tunnel linings were modeled as composite, linear-elastic liners:

- rock support (primary lining) has been modeled as a 'standard beam' characterized by equivalent properties (Table 2). The equivalent section per linear meter comprises a 0.20m thick shotcrete layer (element '2' in figure 4a, b) and double IPN160 ribs spacing 1.5m (element '1' in figure 4a, b). In the model with deformable lining, to simulate the presence of sliding ribs, 4 circumferential sliding slots are considered, each one 0.10m long, thus allowing a circumferential strain of 1.2%;
- the final lining comprises a steel-reinforced concrete section (Tab. 3).
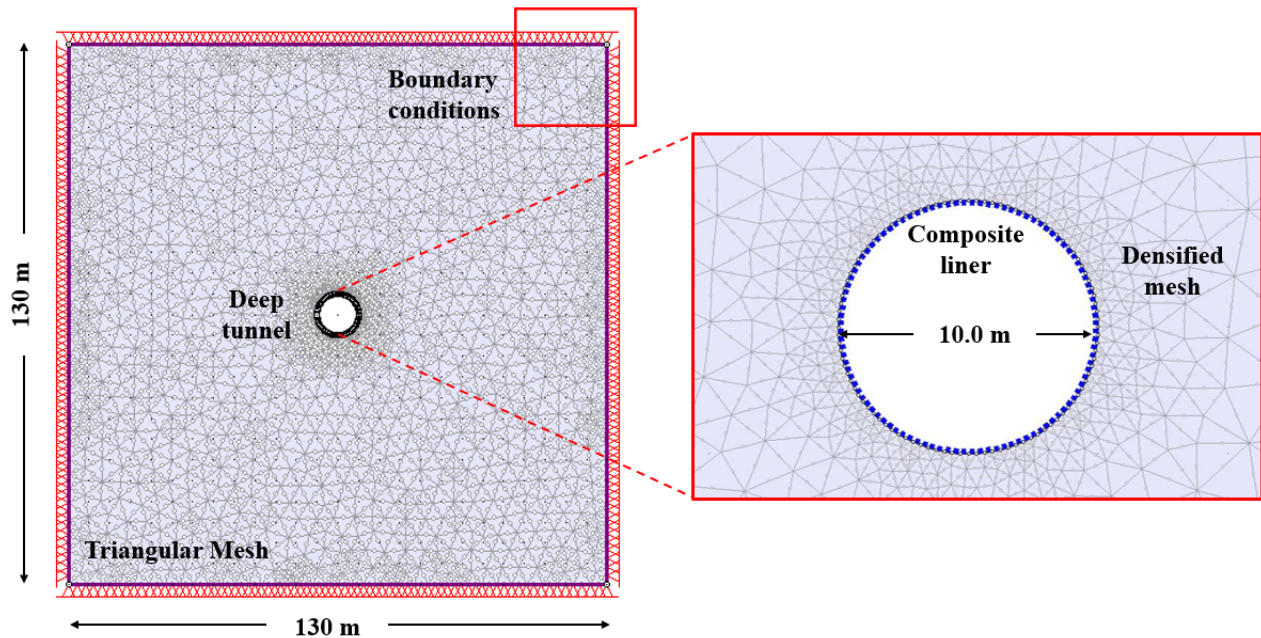
Fig. 3: FE model, geometry, boundary conditions and materials.
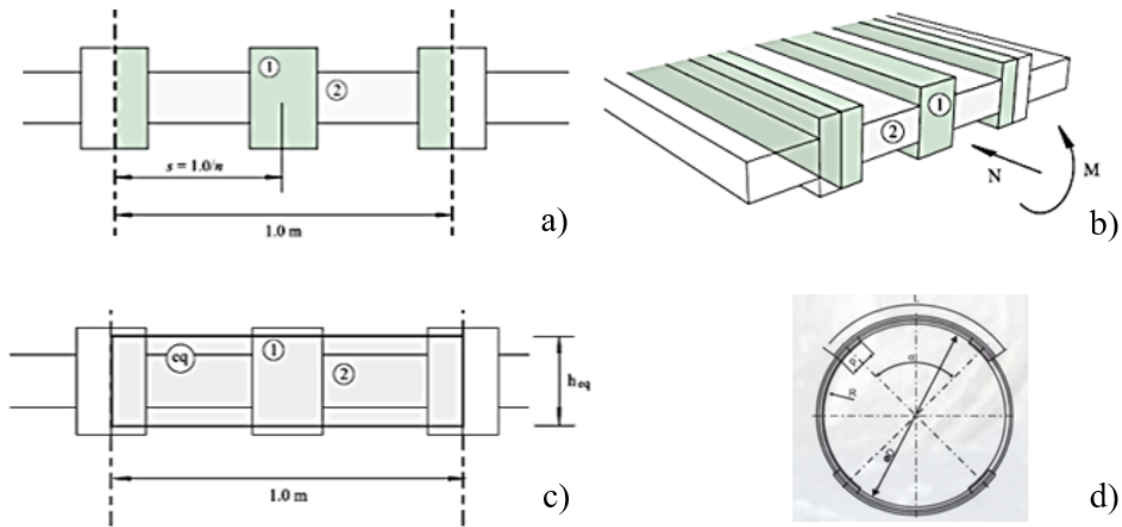
Fig. 4: Rock support section made of IPN ribs and shotcrete layer (a, b), equivalent section (c), and example of transversal section equipped with sliding ribs.

Table 2: Equivalent rock support parameters: elastic modulus (E_{eq}), thickness (h_{eq}), area (A_{eq}), inertia (I_{eq}), Poisson's ratio (v), circumferential strain (ε_c).

	E_{eq} [MPa]	h_{eq} [m]	A_{eq} [m²]	I_{eq} [m⁴]	v [-]	ε_c [%]
Rock support type A: stiff ribs	4435	0.21	0.215	0.000826	0.20	-
Rock support type B: sliding ribs	4435	0.21	0.215	0.000826	0.20	1.2

Table 3: Final lining parameters: elastic modulus (E), spacing (s), diameter (Φ), rebar depth (d), thickness (h), area (A), inertia (I), Poisson's ratio (v), compressive strength (σ_c), tensile strength (σ_t).

	E [GPa]	s [m]	Φ [mm]	d [mm]	h [m]	A [mm²/m]	I [m⁴]	v [-]	σ_c [MPa]	σ_t [MPa]
Reinforcement (rebar B450C, 2 layers)	200	0.25	16	0.9	-	803 x 2	8.14·10⁻⁵	0.25	450	450
Concrete C20/25	30	-	-	-	1.0	-	-	0.15	25	3

2.2. Design methodology

Finite element analyses are carried out to investigate the safety level depending on the type of rock support, respectively stiff ribs or sliding ribs, as follows:

- a preliminary Convergence-Confinement bidimensional analysis of the unsupported tunnel is carried out by performing 10 calculation stages (p_i/p_0=1.0, p_i/p_0=0.8, p_i/p_0=0.4, p_i/p_0=0.2, p_i/p_0=0.1, p_i/p_0=0.08, p_i/p_0=0.04, p_i/p_0=0.02, p_i/p_0=0.01 and p_i/p_0=0). The maximum convergence (u_{max}) and the plastic radius (R_P) of the unsupported tunnel at the final step are obtained (Fig.5b);

- the method proposed by [11] allowed obtaining the tunnel convergence (u_r) at the relevant distances from the tunnel face (i.e. tunnel face: X=0m; installation of the rock support: X=1m) by knowledge of the ratio R_P/R_T, as shown in figure 5a;
- according to the convergence-confinement method ([12]), radial displacements allowed obtaining the ratio p_i/p_0=(1-λ) at the tunnel face and rock support installation, so obtaining the relaxing factor λ(X) as provided in Fig.5b;
- knowledge of the relaxing factors allowed the carrying out of a second series of FE analyses made of two models to compare the different rock supports. Each model, performed at GSI=25-45 (analysis n.1 → analysis n.5), was conducted through 7 calculation stages as detailed in Table 4.
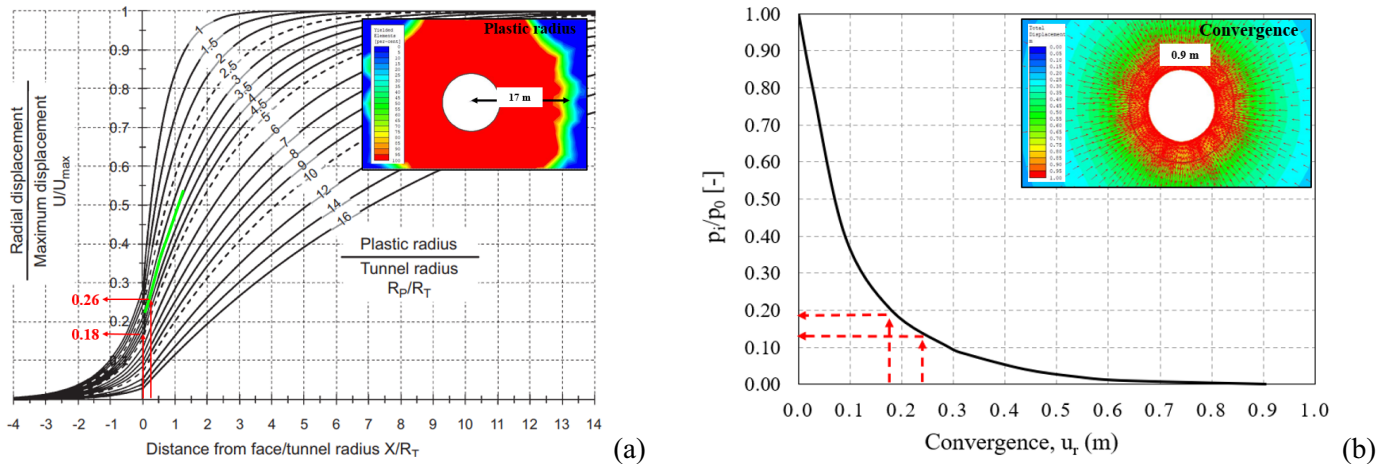
Fig. 5: Analysis n.3 (GSI=35) - (a) solution proposed by [11] to estimate the tunnel convergence and different tunnel face distances, and plastic radius of the unsupported tunnel; (b) evaluation of the ratio p_i/p_0, and so the relaxing factor from the ground reaction curve.

Table 4: Finite element model steps and description.

Step n.	p_i/p_0 (X)	Description
1	1.0	in-situ state of stress
2	p_i/p_0 (X=0.0m)	tunnel face excavation, distance X=0.0m
3	p_i/p_0 (X=1.0m)	temporary lining installation, tunnel face distance, X=1.0m
4	p_i/p_0 (X=2.0m)	tunnel excavation advance, tunnel face distance, X=2.0m
5	p_i/p_0 (X=5.0m)	shotcrete curing at 5 days, tunnel face distance, X=5.0m
6	p_i/p_0 (X=10.0m)	shotcrete curing at 7 days, tunnel face distance, X=10.0m
7	0.0	final lining installation, far from the tunnel face distance, X=20.0m

3. Results

A comparison between numerical results obtained from FE analyses considering rock support type A (stiff ribs) or type B (sliding ribs) is provided in Table 5 in terms of maximum convergence at final lining installation (u), plastic radius (R_P), characteristic values of the maximum axial force (N_{max}) and maximum bending moment (M_{max}). Numerical outputs are provided with their characteristic values (analyses performed under GSI=35), as shown in Fig. 6-9.

Table 5: Comparison between stiff and sliding ribs in terms of maximum convergence at final lining installation (u), plastic radius (R_P), maximum axial force (N_{max}), maximum bending moment (M_{max}).

Analysis	E_d [MPa]	GSI [-]	Rock support type A: stiff ribs				Rock support type B: sliding ribs			
			u [m]	R_P [m]	N_{max} [MN]	M_{max} [kNm]	u(X=2D) [mm]	R_P [m]	N_{max} [MN]	M_{max} [kNm]
1	395	25	0.53	10.50	12.10	5.00	1.13	15.00	2.94	20.00
2	537	30	0.39	10.10	9.80	3.50	0.68	13.20	3.30	16.00
3	750	35	0.25	9.90	9.31	3.40	0.41	11.70	3.20	12.00
4	1050	40	0.16	8.60	9.20	3.20	0.25	10.40	3.10	9.00
5	1480	45	0.11	8.00	8.30	3.00	0.16	9.90	2.95	7.00
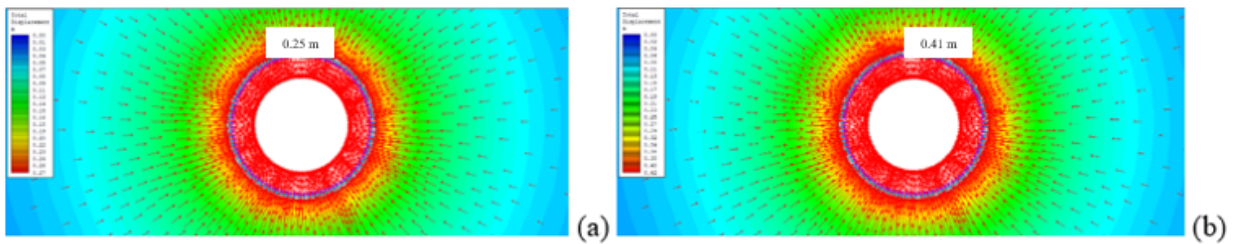
Fig. 6: Analysis n.3 (GSI=35) - maximum tunnel convergence in case of stiff ribs (a), and sliding ribs (b).
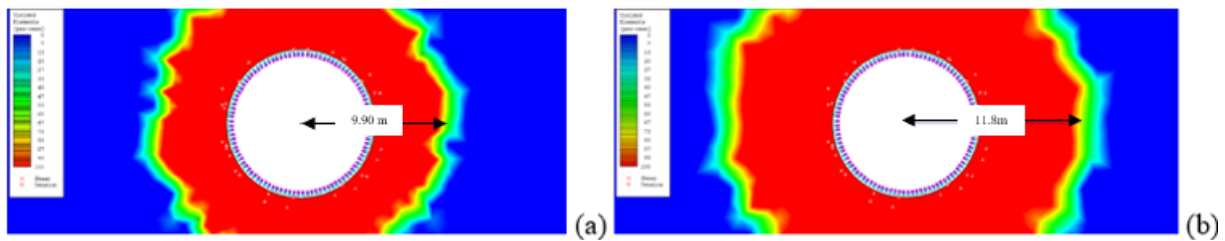
Fig. 7: Analysis n.3 (GSI=35) - plastic radius in case of stiff ribs (a), and sliding ribs (b).
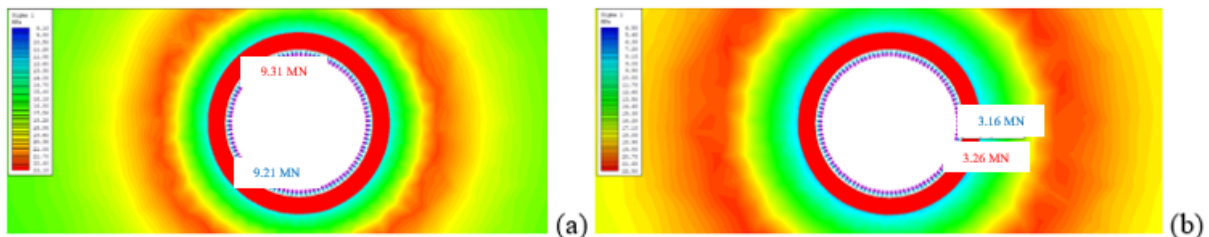
Fig. 8: Analysis n.3 (GSI=35) - axial force in case of stiff ribs (a), and sliding ribs (b).
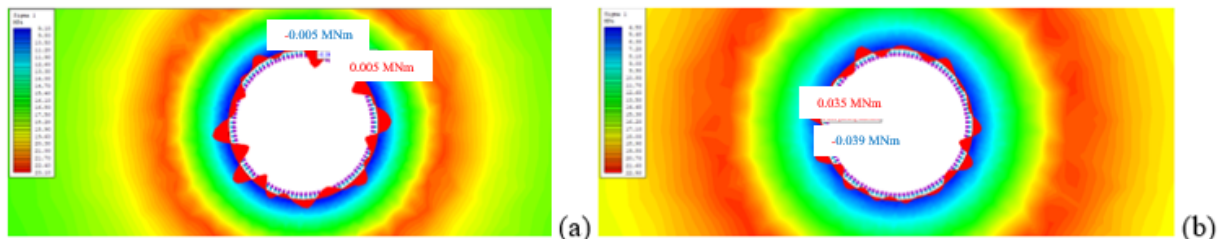
Fig. 9: Analysis n.3 (GSI=35) - bending moment in case of stiff ribs (a), and sliding ribs (b).

The state of stress acting on the rock support type A (red symbols: stiff ribs) and type B (green symbols: deformable ribs) is given in Fig.10a depending on the fracturing state. Because of the isotropic state of stress and the symmetric, circular shape of the tunnel, bending moments assume low values if compared to the axial forces acting on the rock supports. For this reason, as a preliminary effort, the safety level has been evaluated by considering the maximum compressive force (N) and its associated bending moment (M). Couples MN are provided with the interaction diagram and the safety level is estimated, as represented in Fig.10b. The fracturing state of the rock mass does not significantly affect the safety level that can be assumed almost constant with GSI. Because of the higher convergences allowed by deformable ribs, they will result in less stressed than stiff ribs, according to Fig.2. Within the analyzed loading conditions, tunnel shape, and state of stress, rock support type B guarantees a higher safety level than stiff ribs when squeezing behavior is expected.

(a)

(b)
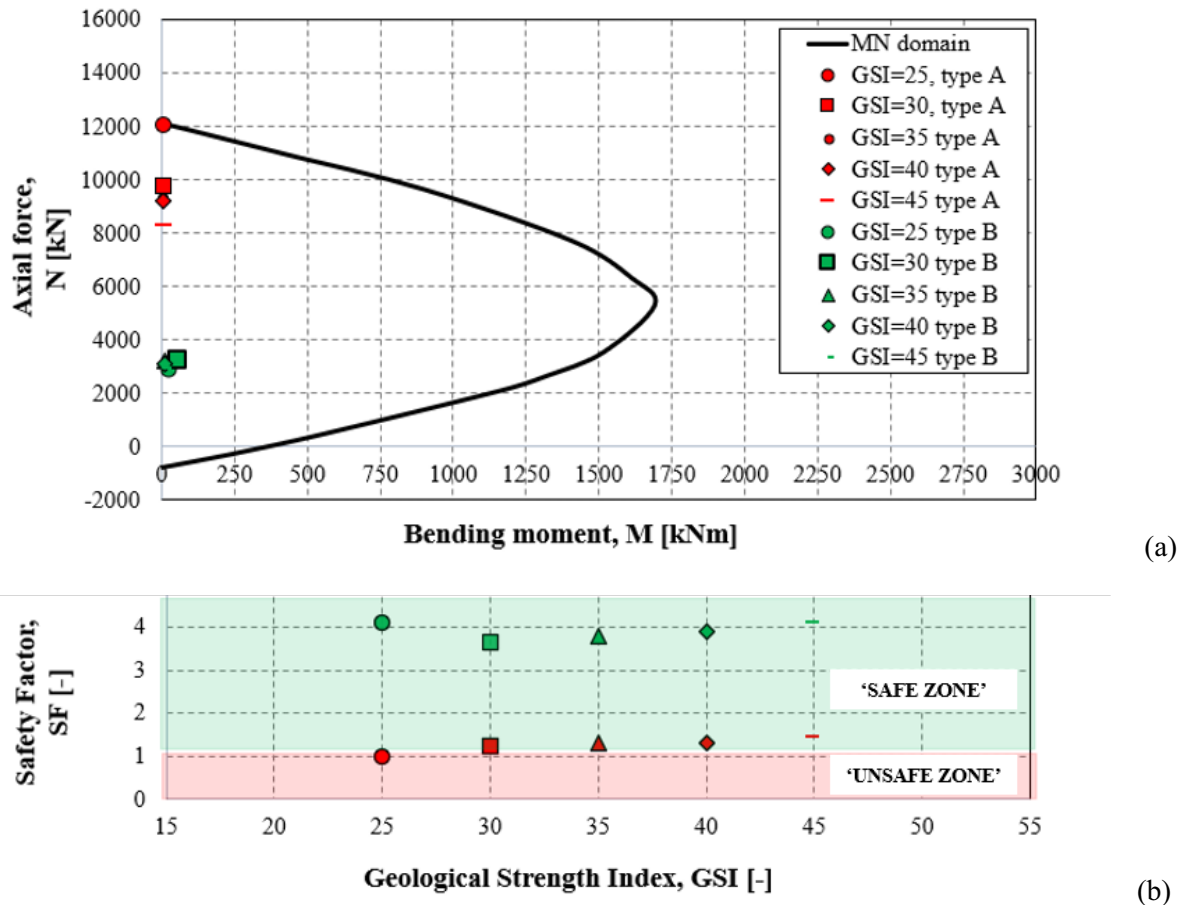
Fig. 10: Comparison between stiff and sliding ribs, (a) MN diagram; (b) safety factor with GSI.

The maximum values of tunnel convergences are provided in Fig.11 in the case of rock support type A (red symbols: stiff ribs) and type B (green symbols: deformable ribs), depending on GSI. In both cases, tunnel convergence decreases when rock mass quality increases (GSI=25 → GSI=45). A higher decrease in GSI is observed in the case of sliding ribs (about 6 times) than stiff ribs (3 times). Differences in convergence are observed for very weak-poor quality rock mass (i.e. GSI=25-35) when stiff or sliding ribs are adopted. On the other side, when dealing with poor-medium rock mass (i.e. GSI=35-45) non-relevant differences can be appreciated in terms of convergence. Of course, no relevant differences are expected for GSI>45 when squeezing behavior could be reasonably excluded because of the medium-good quality of the rock mass.
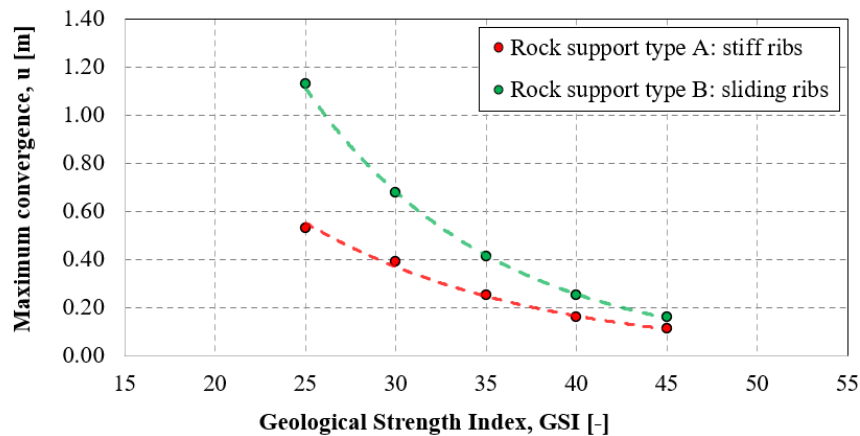
Fig. 11: Maximum convergences when stiff or sliding ribs are applied.

4. Conclusion

An investigation of the stress-strain response of a deep tunnel excavated into a weak rock mass is presented. The safety level in terms of sectional strength and tunnel deformation of different types of rock support is evaluated. Finite element calculations are performed by considering simplified models, thus allowing some preliminary considerations when using stiff or deformable rock support when squeezing behavior is expected. Further analyses could be performed by considering more sophisticated constitutive models allowing take into account the long-time behavior (creep), or the tunnel excavation under an anisotropic state of stress.

References

[1] G. Barla, "Squeezing rocks in tunnels", *ISRM News Journal*, 3/4, pp. 44-49, 1995.
[2] W. Steiner, "Tunnelling in squeezing rocks: case histories", *Rock Mech. and Rock Eng.,* vol. 29, pp. 211-246, 1996.
[3] G. Barla, "Innovative tunneling construction method to cope with squeezing at the Saint Martin La Porte access adit (Lyon-Turin Base Tunnel)", in *Proceedings of the Eurock 2009 Rock Engineering in Difficult Ground Conditions*, Dubrovnik, Croatia, 2009, vol. 1, pp. 1-10.
[4] D. Merlini, D. Stocker, M. Falanesca and R. Schuerch, "The Ceneri Base Tunnel: Construction experience with the Southern Portion of the Flat Railway Line Crossing the Swiss Alps", *Engineering*, vol. 1, no. 2, pp. 235-248, 2018.
[5] N. Radoncic, W. Schubert and B. Moritz "Ductile support design", *Geomechanics and Tunneling*, vol. 2, no.5, 2009.
[6] D.U. Deere, "In Rock Mechanics in Engineering Practice", Eds. Stagg K.G. and Zienkiewicz, O.C., pp. 1-20. London: John Wiley and Sons.
[7] A. Palmstrom and R. Singh "The deformation modulus of rock masses: comparisons between in situ tests and indirect estimates", *Tunnelling and Underground Space Technology*, vol. 16, pp. 115-131, 2001.
[8] E. Hoek and P. Marinos "Predicting tunnel squeezing problems in weak heterogeneous rock masses", *Tunnels and Tunnelling International*, vol. 32, no. 11, pp. 45-51, 2000.
[9] E. Hoek and M.S. Diedrichs, "Empirical estimation of rock mass modulus", *International Journal of Rock Mechanics & Mining Sciences*, vol. 43, pp. 203–215, 2006.
[10] E. Hoek and P. Marinos, "Predicting tunnel squeezing problems in weak heterogeneous rock masses", Tunnels and Tunnelling International, vo. 32, no.11, pp. 45-51, 2000.
[11] N. Vlachopoulos and M.S. Diederichs, "Improved longitudinal displacement profiles for convergence confinement analysis of deep tunnels", *Rock Mechanics and Rock Engineering*, vol. 42, no.2, pp. 131-146, 2009.
[12] M. Panet and A. Guenot, "Analysis of convergence behind the face of a tunnel", in *Proceeding of the International Symposium Tunnelling, (IST'82)*, The Institution of Mining and Metallurgy, London, pp. 197-204, 1982.